VISTA deficiency protects from immune complex-mediated glomerulonephritis by inhibiting neutrophil activation

El Li Tham[1], Simon J Freeley[1], Siobhan Bearder[1], Fernanda Florez Barros[1], Mark S Cragg[2], Attila Mócsai[3], Michael G Robson[1,4]

[1]Department of Inflammation Biology, School of Immunology and Microbial Sciences, King's College London

[2] Antibody and Vaccine Group, Cancer Sciences Unit, Faculty of Medicine, University of Southampton

[3] Department of Physiology, Semmelweis University, School of Medicine, Budapest, Hungary

[4] Corresponding author.
Address: School of Immunology and Microbial Sciences, King's College London,
Guy's Hospital, London SE1 9RT.
Phone 0044 207 188 6768
Michael.robson@kcl.ac.uk
Orchid ID: 0000-0002-1192-1353

Abstract

V-type immunoglobulin domain-containing suppressor of T-cell activation (VISTA) is a negative checkpoint regulator of T cells. We assessed VISTA deficient mice in the murine nephrotoxic nephritis models of acute and chronic immune-complex mediated glomerulonephritis. We show that VISTA deficiency protects from crescentic glomerulonephritis, with no effect on the nephritogenic adaptive immune response. The early neutrophil influx was unaffected but proteinuria was reduced suggesting a reduction in neutrophil activation. In vivo, there was reduced neutrophil degranulation in VISTA deficiency mice and, in vitro, VISTA-deficient neutrophils had an impaired response to immune complexes but not to fMLP or PMA. Mice with a genetic deficiency of neutrophils due to myeloid-specific deletion of myeloid cell leukemia 1 (Mcl-1) were also protected from crescentic glomerulonephritis, indicating an essential role for neutrophils. Therefore, VISTA deficiency inhibits neutrophil activation by immune complexes and neutrophil-dependent crescentic glomerulonephritis. This suggests that VISTA is a therapeutic target for inflammatory disease. However, this would need to be balanced against a potential enhancing effect on autoimmunity.

Keywords: Inflammation, immune complex, glomerulonephritis, neutrophil

1. Introduction

V-region Immunoglobulin-containing Suppressor of T cell Activation is a recently discovered inhibitor of T cell activation. Both in the human and mouse, VISTA expression is restricted to bone marrow derived cells and is highest in myeloid cells (1, 2). VISTA deficient mice have a spontaneous increase in T cell activation although they do not develop spontaneous autoimmunity (3). T cell activation is suppressed by VISTA in models of liver disease and cancer (4-6). VISTA has also been studied in a range of autoimmune disease models using genetic and pharmacological approaches. In both EAE (3) and murine lupus models (7, 8) VISTA blockade or genetic deficiency exacerbates disease. Although VISTA blockade or deficiency has been shown to augment immune-mediated disease via T cell stimulation, it is possible that effects on myeloid cells may dominate in some settings. For example, VISTA blockade is protective in graft versus host disease (1). In addition, VISTA deficiency or blockade affords protection in collagen induced arthritis mediated by passive antibody transfer (9). In both of these studies, it is likely that effects on cells other than T cells are responsible. Therefore, the effect of targeting VISTA may depend on the balance of innate and adaptive immune mechanisms. In some situations, targeting VISTA may have anti-inflammatory effects.

Although it is not autoimmune, the nephrotoxic nephritis models have the advantage of simplicity and they are therefore well suited to mechanistic studies that might help to explain findings in more complex lupus models. Following passive injection of glomerular-binding (nephrotoxic) antibody, there is a neutrophil influx that peaks at 2 hours and is largely resolved by 24 hours, leading to proteinuria. This is known as the heterologous phase of the nephrotoxic nephritis model (10, 11). Following this, progressive disease occurs due to the murine immune response to sheep IgG, which acts as a foreign antigen planted in the glomerulus. Immunisation with sheep IgG, prior to nephrotoxic antibody may be used to augment disease. This is known as the autologous phase of the nephrotoxic nephritis model (12) (13). Histological changes are similar to inflammatory glomerulonephritis in patients, with crescent formation, thrombosis, and monocyte/macrophage infiltration. These changes occur without the need to generate an autoimmune response. Over several decades, studies in this model have shown the role of complement, Fc receptors, cytokines, chemokines, adhesion molecules in renal disease. It has also been used to directly

assess factors leading to kidney damage in lupus-prone mice (14). Thus, the model is relevant to our understanding of mechanisms in lupus nephritis and other forms of immune complex glomerulonephritis.

We studied VISTA deficient mice in both the autologous and the heterologous phase of the nephrotoxic nephritis model and observed protection from disease in both. We also found that neutrophil activation is defective in VISTA deficient mice and that neutrophils were essential in the autologous nephrotoxic nephritis model.

2. Methods

2.1 Mice

VISTA deficient mice were obtained from the Mutant Mouse Regional Resource Centre (15). They were backcrossed at least 10 generations to C57BL/6J. Wildtype C57BL6/J mice were from Charles River UK. C57BL/6 mice congenic for CD45.1 (B6.SJL-*Ptprc*^{a} *Pepc*^{b}/BoyJ) were obtained from the Jackson laboratory. Bone marrow recipients were heterozygous for CD45.1, obtained by breeding with wildtype C57BL6/J mice. LysMcre/creMcl1flox/+ were bred in Semmelweis University, Budapest to generate Lyz2$^{Cre/Cre}$Mcl1$^{flox/flox}$ or Lyz2$^{Cre/Cre}$Mcl1$^{flox/+}$ mice (16, 17). Male mice were used as bone marrow donors and called Mcl1$^{\Delta Myelo}$ and controls respectively. Mice used for in vivo experiments were all male, age-matched and aged 8-12 weeks. For in vitro experiments tissue from both male and female mice was used with age and genders matching in all cases. All experiments were performed according to local and UK home office regulations.

Induction of autologous and heterologous nephrotoxic nephritis

Autologous nephrotoxic nephritis was induced in wild type and VISTA deficient mice as described. Mice were immunized subcutaneously with 200ug sheep IgG, prepared in house with DEAE sepharose (13), in complete Freund's complete adjuvant (Sigma). Five days later they were given an intravenous injection of nephrotoxic serum (150ul/20g), prepared by immunizing sheep with a

mouse kidney preparation as described (13). Heterologous nephrotoxic nephritis was induced as described with a single intravenous injection of nephrotoxic serum (200ul/20g) (18) (19). Functional and histological assessment of disease, and the immune response to sheet IgG is described in supplementary methods.

2.3 Functional and histological assessment of disease in nephrotoxic nephritis

Urine albumin was measured by ELISA with capture and detection antibodies from Bethyl laboratories, and mouse albumin from Sigma to generate a standard curve. In the heterologous model mice were placed in metabolic cages and total urinary albumin per day calculated from the volume and concentration. For the autologous model spot urines were collected and urine albumin creatinine ratios calculated. Serum creatinine was measured using mass spectrometry in the paediatric biochemistry department at Guy's and St Thomas' NHS Trust.

Kidney was fixed in Bouin's solution and stained with PAS. With the exception of Figure 3E, neutrophils were identified by their characteristic morphology on PAS-stained sections. On PAS-stained sections, a minimum of 50 glomeruli per sample were assessed. Neutrophils are reliably identified by light microscopy and more glomeruli are usually available for assessment on paraffin embedded sections. We have previously demonstrated a close correlation with numbers obtained by immunofluorescence staining of phosphate-Lysine periodate (PLP) fixed tissue (25). PLP fixed tissue was used for immunofluorescence with a minimum of 30 glomeruli (Figure 3E) or 20 glomeruli (Figure 1D-E and Figure 5D) per sample assessed. For Figure 3E, staining for Ly6G was used to identify neutrophils in order to allow assessment of the same samples in which MPO deposits were identified. Unlabelled primary antibodies were CD68 (clone FA1, Serotec), CD4 (L3T4, BD Biosciences), Ly6G (clone 1A8, BioLegend), myeloperoxidase (clone BF4,Hycult Biotech). Detection was with Dylite 488 conjugated mouse anti-rat IgG, (Jackson's Immunoresearch). All histological assessments were performed by a blinded researcher without knowledge of the sample identity. The humoral immune response to sheep IgG was measured using subclass-specific ELISAs as described previously (20). Single cell suspensions were prepared from spleens and resuspended at $4x10^6$ /ml in X-vivo 15 medium (Lonza) with 1%

glutamax, and 50uM beta-mercaptoethanol. Spleen cells from each mouse were cultured with and without 100ug/ml sheep IgG for 5 days. IFNγ and IL-17 were measured by ELISA (R and D).

2.4 Nanostring assay

RNA was extracted from snap frozen tissue using a TissueLyser and RNAeasy (Qiagen). The Nanostring assay was run in the core facility at Dartmouth using the mouse immunology panel.

2.5 Bone marrow transplantation

Bone marrow transplants were performed as described (13) (21). Legs from donor mice were sent from Semmelweis University, Budapest to King's College London, and bone marrow cells extracted within 24 hours of death. Recipient mice were irradiated with a dose 9Gy using a caesium-137 source and reconstituted with 10 x 10^6 donor cells, injected intravenously on the same day.

2.6 Whole blood leukocyte staining

Staining for flow cytometry was performed on whole blood taken from the saphenous vein. Antibodies used were CD45.1 (clone A20, BioLegend), CD45.2 (clone104, ThermoFisher), CD11b (clone M1/70, eBioscience), Ly6C (clone AL-21, BD), Ly6G (clone 1A8, BioLegend). Facs lysing solution (BD biosciences) was used prior to analysis. The same antibodies were used for whole blood staining of baseline samples from VISTA deficient and control mice and from bone marrow chimeras 10 weeks after bone marrow engraftment. Samples were run on a BD Fortessa flow cytometer and data analysed using Flowjo software. Total white counts were obtained using a haemocytometer and EDTA anticoagulated blood diluted in Turk's solution.

Neutrophil activation assays

Neutrophils were obtained from the bone marrow of wild type and VISTA deficient mice using a negative selection kit (Miltenyi, Bisley, UK) according to instructions, and suspended in RPMI and 10% FCS (both Sigma, Poole). Plate bound Immune complexes were made from HSA and polyclonal rabbit anti-HAS (both from Sigma). HAS (20 µg/ml) in 50 mM carbonate/bicarbonate

buffer (pH 9.6) was coated overnight at 4'C in 96 well plates. After washing they were blocked with HSA and incubated with anti-HSA for one hour at room temperature, followed by washing. Isolated neutrophils are resuspended in PBS++ (Sigma) and mixed with luminol/HRP. Luminol 0.33mM and HRP 50 U/ml was prepared mixed with the neutrophil suspension at a ratio of 1.25:1. The final concentration of neutrophils was 1 x 10^6/ml. Neutrophils mixed with luminol and HRP were added to wells coated with immune complexes. In some experiments, cells were stimulated with 5ug/ml cytochalasin B, 10uM fMLP or 300mM PMA (all from Sigma). Luminescence was read using SpectraMax MiniMax 300 plate reader (Molecular devises) at 30 seconds (immune complexes) or 8 seconds (fMLP or PMA) intervals. Elastase was measured using an enzymatic assay (Molecular Probes) or by ELISA (R&D) according to instructions.

2.7 Flow Cytometric analysis of Fcγ receptors.

Whole blood or bone marrow cells were taken from wild type and VISTA deficient mice and stained for the following: CD11b (clone M1/70, eBioscience), CD45 (clone 30-F11, BioLegend), CD19 (clone 1D3, BD), Ly6C (clone AL-21, BD), Ly6G (clone 1A8, BioLegend). For Fcγ receptor staining, reagents generated and FITC labelled in house were; FcγRI (AT152-9, Fab_2) and FcγR III (AT154-2 Fab_2), and FcγR IIb (AT130-2 N297A and Fab_2). FcγR IV was detected with 9E9 provided by J Ravetch and FITC labelled in house. Control staining was performed with MC106A5 Fab_2 or 4D5-N297A IgG as indicated. Samples were run on a BD LSR Fortessa II flow cytometer and data analysed using Flowjo software.

2.8 Kidney digestion with flow cytometry.

Kidneys were finely chopped in HBSS supplemented with 3mg/ml collagenase/dispase, 0.2mg/ml DNase type 1 and 50 μm $CaCl_2$ (all from Sigma). After 20 minutes of agitation at 37'C they were passed through 70um and 40um cell strainers, incubated with red cell lysis buffer (BD biosciences) prior to flow cytometry. Antibodies used for flow cytometry were as follows: Ly6G (clone 1A8, BD Pharmingen), CD63 (clone NVG-2, BioLegend). Samples were run on a BD Fortessa flow cytometer and data analysed using Flowjo software.

2.9 Statistics

To analyze the NanoString data, gene expression data from NanoString were normalized in nSolver and log_2-transformed for further analysis for differential expression. Data were analyzed in R using unpaired *t* tests followed by Benjamini and Hochberg multiple hypothesis correction. Gene expression values were normalized to the geometric mean of housekeeping genes using nSolver software (NanoString Technologies). For all other data, Graphpad Prism version 7 was used. Where two groups were compared, a student's t test was used, with data logarithmically transformed if there was a significant difference between variances. Exceptions to this are the neutrophil activation data in Figure 4A, and the analysis for N297A anti-FcγRIIb in Figure S2, where a two-way ANOVA was used (as indicated in the figure legend).

3. Results

3.1 VISTA deficiency protects from crescentic glomerulonephritis

We compared VISTA deficient mice with wild type mice in autologous nephrotoxic nephritis. Thrombosis, crescent formation and glomerular CD68 positive cells were reduced in VISTA deficient mice (Figure 1A-D). There were no differences in infiltrating CD4+ T cells (Figure 1E). Functional measures of renal disease include serum creatinine and albuminuria. Serum creatinine was significantly lower in VISTA deficient mice than wild type mice, indicating preserved in renal function (Figure 1F). Baseline serum creatinine was similar at 7.5+3.1 and 8.2±0.73 umol/L in wild type and VISTA deficient mice respectively. We did not detect a difference in urine albumin creatinine ratio (Figure 1G). Baseline urine albumin creatinine ratios were similar 5.4±0.46 and 4.9±0.48 mg/mmol in wild type and VISTA deficient mice respectively. These were approximately 1000 times lower than levels seen after disease induction. Overall, we found that VISTA deficient mice were protected from crescentic glomerulonephritis by histological parameters and with preservation of renal function.

We performed a transcriptional analysis of renal cortex using a Nanostring immunology panel and found differential expression of multiple genes (Figure S1). In total 49 genes had a difference of more than 2-fold with an adjusted p value of <0.05. 47 genes showed a lower expression in VISTA

deficient mice than wildtypes. Many of these genes, such as CD44, Fcgr3, FcgR4, Csf2rb, CD14, Trem,Trem2, IL18rap, IL10ra, IL2ra, CD109 and CD163 are expressed primarily on leukocytes and probably reflected a decrease in leukocyte infiltration. Soluble proteins with decreased expression included IL1-beta, ccl6, ccl9 and cxcl1. Overall these data provide further evidence of protection from inflammation and disease in VISTA deficient mice.

3.2 VISTA deficiency does not affect the immune response to sheep IgG or circulating leukocyte numbers

We assessed the humoral response using subclass-specific ELISAs and no differences were found (figure 2A). We also assessed the antigen-specific T cell response using spleen cells taken at the end of the experiment (figure 2B). Again, no differences were found. Baseline numbers of circulating monocytes and neutrophils were similar in wild type and VISTA deficient mice (Figure 2C). The Nanostring immunology panel included IFNγ and IL-17A and IL17-F (Figure 2D). There was a reduction in IFNγ in VISTA deficient mice which reached statistical significance but was small in magnitude, with no differences in IL-17A or IL-17F. Together with the similar number of infiltrating CD4+ T cells (Figure 1E), these data further suggest that protection from disease was due to an effect on innate rather than adaptive immunity.

3.3 VISTA deficiency protects from proteinuria but not neutrophil recruitment

We assessed the effect of VISTA deficiency on the early neutrophil influx in heterologous nephrotoxic nephritis. We found that there was no difference in the number of glomerular neutrophils at 2 hours in VISTA deficient mice compared to wild types (Figure 3A). A further experiment showed there was no difference in neutrophil numbers at the later time point of 4 hours (Figure 3B). However, despite a similar degree of neutrophil influx, there was less albuminuria in VISTA deficient mice (Figure 3C). Baseline albuminuria was similar in both groups, and far lower than in diseased mice. Levels were 38±6.4 and 45±2.9 (μg/day : mean+SEM) for wild type and VISTA deficient mice respectively. Since proteinuria is known to depend on neutrophil activation (10) these data suggested a defect in neutrophil activation due to VISTA deficiency. Representative glomeruli are shown in Figure 3D. As a marker of neutrophil degranulation over

the first 24 hours, we measured glomerular deposition of myeloperoxidase (MPO), which is found in neutrophil primary granules (22) . Following neutrophil activation, MPO is a key component of neutrophil extracellular traps (NETs) (23). Few neutrophils remain in glomeruli at 24 hours in this model. On the same samples, we used immunofluorescence staining for Ly6G to assess if any differences in the number of myeloperoxidase deposits seen were due to differences in neutrophil numbers. There was no difference in neutrophil numbers, but there was less myeloperoxidase found in the glomeruli of VISTA deficient mice. Data are shown in Figure 3E with representative immunofluorescent staining in Figure 3F. These findings suggested that the decrease in albuminuria was associated with reduced neutrophil activation and NETosis in VISTA deficient mice.

3.4 Vista deficiency inhibits neutrophil activation by immune complexes

The respiratory burst was significantly decreased in VISTA deficient neutrophils stimulated by immune complexes. However, the response to fMLP and PMA was similar in VISTA deficient and wild type mice (Figure 4A). Luminescence over time in response to immune complexes is shown in Figure 4B for one experiment. We assessed degranulation after stimulation with fMLP by measuring soluble elastase and cell surface CD63 expression. CD63 is contained in primary granules and increases on the plasma membrane with degranulation. There were no differences in either case (Figure S2 A-B). We also measured elastase after stimulation with immune complexes. However, a high background level of degranulation was seen over the longer time course of activation. Immune complexes did not cause an increase in elastase above background. This is shown in Figure S2C, which further confirms the lack of difference in elastase release for VISTA deficient compared to wild type mice in response to fMLP. Since the in vitro assay was not suitable for assessing degranulation in response to immune complexes, we measured CD63 expression on neutrophils in kidney digests taken at 2 hours in the nephrotoxic nephritis model. This offered a direct assessment of neutrophil degranulation in vivo. As shown in Figure 4C, cell surface CD63 was decreased in neutrophils from VISTA deficient mice compared to wild types demonstrating less degranulation in vivo.

3.5 Fcγ receptor expression

Flow cytometry of bone marrow and peripheral blood from wild type and VISTA deficient mice is shown in Figure S3A. Initial data in bone marrow neutrophils suggested a small difference in FcγRIIb expression (Figure S3D). Therefore, we performed a second experiment. This second experiment included staining with both Fab_2 antibodies and IgG with a mutated Fc region to minimize Fcγ receptor interactions (N297A) with controls. This second experiment showed no differences. For the data using the N297A anti-FcγRIIb antibody, a combined analysis of the two experiments using a two-way ANOVA showed no significant difference. Overall the data show no substantial and reproducible differences in expression of any Fcγ receptors in blood or bone marrow neutrophils.

3.6 Neutrophils are required for crescentic glomerulonephritis

Next, we considered if the protection from crescentic glomerulonephritis in the autologous nephrotoxic nephritis model could be explained by an effect on neutrophils. We used $Mcl1^{\Delta Myelo}$ mice which are selectively deficienct in neutrophils (16, 17). Bone marrow from control or $Mcl1^{\Delta Myelo}$ mice was transplanted into recipients heterozygous for CD45.1. This approach was taken due to the limited availability of $Mcl1^{\Delta Myelo}$ mice, and to avoid the need to transfer live animals between collaborating centres. Flow cytometry on whole blood for CD45.1, CD45.2, Ly6C, CD11b and Ly6G was taken at baseline to assess chimerism, and numbers of circulating leukocytes during the experiment. The gating strategy is shown for a mouse receiving control marrow or $Mcl1^{\Delta Myelo}$ marrow in figure S4A and S4B respectively. As expected, there were few Ly6G+ neutrophils seen in recipients of $Mcl1^{\Delta Myelo}$ marrow (Figure S4B). At baseline, CD45.2+CD45.1- donor derived monocytes and neutrophils were assessed as a percentage of total CD45+. More than 99% of circulating monocytes (Ly6C+Ly6G-CD11b+ cells) were donor derived in all mice. In addition, with the exception of one mouse receiving $Mcl1^{\Delta Myelo}$ marrow, more than 93% of circulating neutrophils were donor derived. These data on the degree of chimerism are shown in Figure S4C. Autologous nephrotoxic nephritis was induced as before.

Blood was again taken from the saphenous vein at day one and day 5 after disease induction. Peripheral blood neutrophils and monocyte numbers were calculated from a manual total white blood cell count and the percentage of total CD45+ cells that were CD11b+Ly6G+ or CD11b+Ly6C+Ly6G- respectively. Mcl1$^{\Delta Myelo}$ mice had lower neutrophil levels at baseline and throughout the experiment (Figure S4D), with no difference in monocyte numbers (Figure 5E). Mice were killed 11 days after injection of nephrotoxic serum. Mcl1$^{\Delta Myelo}$ mice demonstrated less glomerular thrombosis and fewer crescents and CD68+ macrophages (Figure 5A-D). Serum creatinine and albuminuria were also reduced in Mcl1$^{\Delta Myelo}$ mice (Figure 5E-F). There were no differences in baseline levels. Serum creatinine before disease induction was 7.9±0.57 and 7.3±0.62 umol/L in wild type and Mcl1$^{\Delta Myelo}$ mice respectively, with urine albumin creatinine ratios of 2.1±0.24 and 1.8±0.29 mg/mmol respectively. Levels of antigen-specific IgG1 and IgG2b were higher in Mcl1$^{\Delta Myelo}$ mice showing that the difference in disease severity was not due to a difference in the immune response to sheep IgG (Figure S5). These data show that neutrophil deficient Mcl1$^{\Delta Myelo}$ mice are protected from crescentic glomerulonephritis. Therefore, neutrophils are required for crescentic glomerulonephritis in the autologous nephrotoxic nephritis model. This suggests that a defect in neutrophil activation, present in VISTA deficient mice, could explain the protection from disease in this model.

4. Discussion

The protection that we have shown here in VISTA deficient mice in the nephrotoxic nephritis model is in contrast to the augmented disease seen in lupus-prone *Sle1.Sle3* mice mice with VISTA deficiency or blockade (8). Although in *Sle1.Sle3* mice mice with VISTA deficiency there was no difference in anti-dsDNA antibodies, there was an increase in splenic T cell activation and in pro-inflammatory cytokines in both serum and splenic myeloid cells (8). Treatment with VISTA blockade in the lupus prone (NZBxNZW) F1 mice also increased glomerular inflammation and proteinuria, with an increase in splenic T cell activation but no difference in anti-dsDNA antibodies (7). Hence, VISTA deficiency or blockade accelerates murine lupus without modifying autoantibody

levels, in association with effects on T cell activation and systemic cytokine levels. Despite the lack of effect on autoantibodies, the enhanced T cell and splenic myeloid cell activation in lupus-prone mice may have overshadowed any protective effects on neutrophil activation. This illustrates the complexity of lupus models and the difficulty in understanding the mechanisms of observed effects. The autologous nephrotoxic nephritis model is not autoimmune and avoids these complexities. As there was no effect on the immune response to sheep IgG we can assume that protection was due to inhibition of innate inflammatory mechanisms.

Results in the passive transfer collagen-induced arthritis model are in keeping with the data we present here, since VISTA deficient mice are also protected (9). This is another example of protection from an immune complex-mediated disease. Disease is induced by passive transfer of arthritogenic antibody and thus any observed differences in disease reflect differences in innate immunity. VISTA deficient macrophages showed altered activation due to immune complexes, with an increase in IL1 receptor antagonist. There was also a decrease in C5a receptor expression in neutrophils, monocytes and macrophages. A decrease in C5a receptor expression is unlikely to explain our findings in the heterologous nephrotoxic nephritis model. This is a chemotaxis receptor and neutrophil influx was similar in both groups. Neutrophils are thought to be essential for disease in collagen induced arthritis. (24, 25) and in disease induced by K/B×N serum transfer (26). Hence, the diminished response in VISTA deficient neutrophils to immune complexes that we have shown is also likely to contribute to protection in collagen-induced arthritis, in addition to effects on macrophages. Conversely, a decrease in anti-inflammatory gene expression in VISTA-deficiency macrophages may have also contributed to the protection we observed in the autologous nephrotoxic nephritis model.

We have also directly shown an essential role for neutrophils in crescentic glomerulonephritis Previous data have indirectly supported a role for neutrophils in autologous nephrotoxic nephritis. The transgenic expression of human Fcγ receptors exclusively on neutrophils was sufficient to reconstitute disease in autologous nephrotoxic nephritis (27). In another report, neutrophils were depleted in the autologous nephrotoxic nephritis model using an antibody to Ly6G (28). Although

effects on histology were suggested, there was no reported effect on renal function or proteinuria, perhaps due to the small number of animals used (n=4 per group). A further publication in the murine anti-myeloperoxidase model of vasculitis suggested that neutrophil depletion was protective (29). However, in this study the monoclonal antibody used (NIMP-R14) would also have depleted monocytes and a specific role for neutrophils was not unequivocally shown. Overall there have been no previous data that directly show a requirement for neutrophils in crescentic glomerulonephritis. In some forms of human glomerulonephritis including anti-neutrophil cytoplasmic antibody vasculitis, there is evidence that neutrophils undergo NETosis and deposit chromatin in glomeruli (30). Previous work in the murine nephrotoxic nephritis model has shown a beneficial effect from both blockade of NET formation and administration of anti-histone IgG (31). The reduced MPO deposition that we saw in VISTA deficient mice probably reflects decreased NETosis. Therefore, it seems likely that NETosis makes an important contribution to the pathogenic effects mediated by neutrophils.

In previous work, $Mcl1^{\Delta Myelo}$ mice were studied in the pristane-induced lupus model (32). Proteinuria was not affected by neutrophil deficiency suggesting neutrophils were not required for glomerular disease. However, there was no histological assessment of disease in this study. In addition, interpretation was complex, because autoimmunity was enhanced in the absence of neutrophils. A decrease in tendency downstream inflammation could have been offset by the increase in autoimmunity. We saw an increase in IgG1 and IgG2b antibody against sheep IgG, suggesting that humoral response to foreign antigens is also increased in $Mcl1^{\Delta Myelo}$ mice. The reason for this is not clear but protection from renal inflammation occurred despite this enhanced adaptive immunity.

The requirement for neutrophils in crescentic glomerulonephritis suggests that the defective neutrophil activation seen in VISTA deficient mice, in response to immune complexes in vitro and in the heterologous phase in vivo, also accounts for the protection from crescentic glomerulonephritis with VISTA deficiency. However, it is possible that a defect in activation of

other myeloid cells such as macrophages, as discussed in the context of the results in the collagen-induced arthritis model (9), also contributed to protection from glomerular disease.

In conclusion, VISTA deficiency inhibits neutrophil activation by immune complexes and protects from neutrophil-dependent immune complex-mediated glomerular inflammation. This suggests that VISTA blockade may be an effective anti-inflammatory therapy. However, this would need to be balanced against a potential enhancing effect on autoimmunity (7).

5. Conclusions

VISTA deficiency inhibits neutrophil activation by immune complexes and neutrophil-dependent crescentic glomerulonephritis. This suggests that VISTA is a therapeutic target for inflammatory disease, although effects on both inflammation and autoimmunity will need to be considered.

6. Acknowledgments

We are grateful for Randolph Noelle and Sabrina Ceeraz (Geisel School of Medicine at Dartmouth, Lebanon, New Hampshire, USA) for coordinating the Nanostring assay and analysis. We are also grateful to Randolphe Noelle for the VISTA deficient mice, and for helpful discussion. Preliminary work was funded by Immunext Inc. The authors have no other disclosures. This work was supported by grants from Kidney Research UK (RP1/2015) and Immunext Inc. Additional support was from the Medical Research Council (MRC) Centre for Transplantation, King's College London, UK – MRC grant no. MR/J006742/1 and the National Institute for Health Research (NIHR) Biomedical Research Centre based at Guy's and St Thomas' NHS Foundation Trust and King's College London. The views expressed are those of the author(s) and not necessarily those of the NHS, the NIHR or the Department of Health.

7. References

1. Flies DB, Wang S, Xu H, Chen L. 2011. Cutting edge: A monoclonal antibody specific for the programmed death-1 homolog prevents graft-versus-host disease in mouse models. J Immunol 187:1537-41.
2. Wang L, Rubinstein R, Lines JL, Wasiuk A, Ahonen C, Guo Y, Lu LF, Gondek D, Wang Y, Fava RA, Fiser A, Almo S, Noelle RJ. 2011. VISTA, a novel mouse Ig superfamily ligand that negatively regulates T cell responses. J Exp Med 208:577-92.
3. Wang L, Le Mercier I, Putra J, Chen W, Liu J, Schenk AD, Nowak EC, Suriawinata AA, Li J, Noelle RJ. 2014. Disruption of the immune-checkpoint VISTA gene imparts a proinflammatory phenotype with predisposition to the development of autoimmunity. Proc Natl Acad Sci U S A 111:14846-51.
4. Flies DB, Higuchi T, Chen L. 2015. Mechanistic Assessment of PD-1H Coinhibitory Receptor-Induced T Cell Tolerance to Allogeneic Antigens. J Immunol 194:5294-304.
5. Flies DB, Han X, Higuchi T, Zheng L, Sun J, Ye JJ, Chen L. 2014. Coinhibitory receptor PD-1H preferentially suppresses CD4(+) T cell-mediated immunity. J Clin Invest 124:1966-75.
6. Le Mercier I, Chen W, Lines JL, Day M, Li J, Sergent P, Noelle RJ, Wang L. 2014. VISTA Regulates the Development of Protective Antitumor Immunity. Cancer Res 74:1933-44.
7. Sergent PA, Plummer SF, Pettus J, Mabaera R, DeLong JK, Pechenick DA, Burns CM, Noelle RJ, Ceeraz S. 2018. Blocking the VISTA pathway enhances disease progression in (NZB x NZW) F1 female mice. Lupus 27:210-216.
8. Ceeraz S, Sergent PA, Plummer SF, Schned AR, Pechenick D, Burns CM, Noelle RJ. 2017. VISTA Deficiency Accelerates the Development of Fatal Murine Lupus Nephritis. Arthritis Rheumatol 69:814-825.
9. Ceeraz S, Eszterhas SK, Sergent PA, Armstrong DA, Ashare A, Broughton T, Wang L, Pechenick D, Burns CM, Noelle RJ, Vincenti MP, Fava RA. 2017. VISTA deficiency attenuates

antibody-induced arthritis and alters macrophage gene expression in response to simulated immune complexes. Arthritis Res Ther 19:270.
10. Schrijver G, Bogman MJ, Assmann KJ, de Waal RM, Robben HC, van Gasteren H, Koene RA. 1990. Anti-GBM nephritis in the mouse: role of granulocytes in the heterologous phase. Kidney Int 38:86-95.
11. Dixon FG, Feldman JD, Vasquez JJ. 1961. Experimental glomerulonephritis: The pathogenesis of a laboratory model resembling the spectrum of human glomerulonephrtis. J Exp Med 113:899-920.
12. Unanue ER, Dixon FJ. 1965. Experimental glomerulonephritis: the autologous phase of nephrotoxic seum nephritis. J Exp Med 121:715.
13. Brown HJ, Lock HR, Sacks SH, Robson MG. 2006. TLR2 stimulation of intrinsic renal cells in the induction of immune-mediated glomerulonephritis. J Immunol 177:1925-31.
14. Xie C, Zhou XJ, Liu X, Mohan C. 2003. Enhanced susceptibility to end-organ disease in the lupus-facilitating NZW mouse strain. Arthritis Rheum 48:1080-92.
15. Tang T, Li L, Tang J, Li Y, Lin WY, Martin F, Grant D, Solloway M, Parker L, Ye W, Forrest W, Ghilardi N, Oravecz T, Platt KA, Rice DS, Hansen GM, Abuin A, Eberhart DE, Godowski P, Holt KH, Peterson A, Zambrowicz BP, de Sauvage FJ. 2010. A mouse knockout library for secreted and transmembrane proteins. Nat Biotechnol 28:749-55.
16. Csepregi JZ, Orosz A, Zajta E, Kasa O, Nemeth T, Simon E, Fodor S, Csonka K, Baratki BL, Kovesdi D, He YW, Gacser A, Mocsai A. 2018. Myeloid-Specific Deletion of Mcl-1 Yields Severely Neutropenic Mice That Survive and Breed in Homozygous Form. J Immunol 201:3793-3803.
17. Weber FC, Nemeth T, Csepregi JZ, Dudeck A, Roers A, Ozsvari B, Oswald E, Puskas LG, Jakob T, Mocsai A, Martin SF. 2015. Neutrophils are required for both the sensitization and elicitation phase of contact hypersensitivity. J Exp Med 212:15-22.
18. Brown HJ, Lock HR, Wolfs TG, Buurman WA, Sacks SH, Robson MG. 2007. Toll-like receptor 4 ligation on intrinsic renal cells contributes to the induction of antibody-mediated glomerulonephritis via CXCL1 and CXCL2. J Am Soc Nephrol 18:1732-9.
19. Robson MG, Cook HT, Pusey CD, Walport MJ, Davies KA. 2003. Antibody-mediated glomerulonephritis in mice: the role of endotoxin, complement and genetic background. Clin Exp Immunol 133:326-33.
20. Giorgini A, Brown HJ, Sacks SH, Robson MG. 2010. Toll-like receptor 4 stimulation triggers crescentic glomerulonephritis by multiple mechanisms including a direct effect on renal cells. Am J Pathol 177:644-53.
21. Freeley SJ, Popat RJ, Parmar K, Kolev M, Hunt BJ, Stover CM, Schwaeble W, Kemper C, Robson MG. 2016. Experimentally-induced anti-myeloperoxidase vasculitis does not require properdin, MASP-2 or bone marrow-derived C5. J Pathol 240:61-71.
22. Oren A, Taylor JM. 1995. The subcellular localization of defensins and myeloperoxidase in human neutrophils: immunocytochemical evidence for azurophil granule heterogeneity. J Lab Clin Med 125:340-7.
23. Brinkmann V, Abu Abed U, Goosmann C, Zychlinsky A. 2016. Immunodetection of NETs in Paraffin-Embedded Tissue. Front Immunol 7:513.
24. Eyles JL, Hickey MJ, Norman MU, Croker BA, Roberts AW, Drake SF, James WG, Metcalf D, Campbell IK, Wicks IP. 2008. A key role for G-CSF-induced neutrophil production and trafficking during inflammatory arthritis. Blood 112:5193-201.
25. Lawlor KE, Campbell IK, Metcalf D, O'Donnell K, van Nieuwenhuijze A, Roberts AW, Wicks IP. 2004. Critical role for granulocyte colony-stimulating factor in inflammatory arthritis. Proc Natl Acad Sci U S A 101:11398-403.

26. Wipke BT, Allen PM. 2001. Essential role of neutrophils in the initiation and progression of a murine model of rheumatoid arthritis. J Immunol 167:1601-8.
27. Tsuboi N, Asano K, Lauterbach M, Mayadas TN. 2008. Human neutrophil Fcgamma receptors initiate and play specialized nonredundant roles in antibody-mediated inflammatory diseases. Immunity 28:833-46.
28. Disteldorf EM, Krebs CF, Paust HJ, Turner JE, Nouailles G, Tittel A, Meyer-Schwesinger C, Stege G, Brix S, Velden J, Wiech T, Helmchen U, Steinmetz OM, Peters A, Bennstein SB, Kaffke A, Llanto C, Lira SA, Mittrucker HW, Stahl RA, Kurts C, Kaufmann SH, Panzer U. 2015. CXCL5 drives neutrophil recruitment in TH17-mediated GN. J Am Soc Nephrol 26:55-66.
29. Xiao H, Heeringa P, Liu Z, Huugen D, Hu P, Maeda N, Falk RJ, Jennette JC. 2005. The role of neutrophils in the induction of glomerulonephritis by anti-myeloperoxidase antibodies. Am J Pathol 167:39-45.
30. Kessenbrock K, Krumbholz M, Schonermarck U, Back W, Gross WL, Werb Z, Grone HJ, Brinkmann V, Jenne DE. 2009. Netting neutrophils in autoimmune small-vessel vasculitis. Nat Med 15:623-5.
31. Kumar SV, Kulkarni OP, Mulay SR, Darisipudi MN, Romoli S, Thomasova D, Scherbaum CR, Hohenstein B, Hugo C, Muller S, Liapis H, Anders HJ. 2015. Neutrophil Extracellular Trap-Related Extracellular Histones Cause Vascular Necrosis in Severe GN. J Am Soc Nephrol 26:2399-413.
32. Kienhofer D, Hahn J, Stoof J, Csepregi JZ, Reinwald C, Urbonaviciute V, Johnsson C, Maueroder C, Podolska MJ, Biermann MH, Leppkes M, Harrer T, Hultqvist M, Olofsson P, Munoz LE, Mocsai A, Herrmann M, Schett G, Holmdahl R, Hoffmann MH. 2017. Experimental lupus is aggravated in mouse strains with impaired induction of neutrophil extracellular traps. JCI Insight 2.

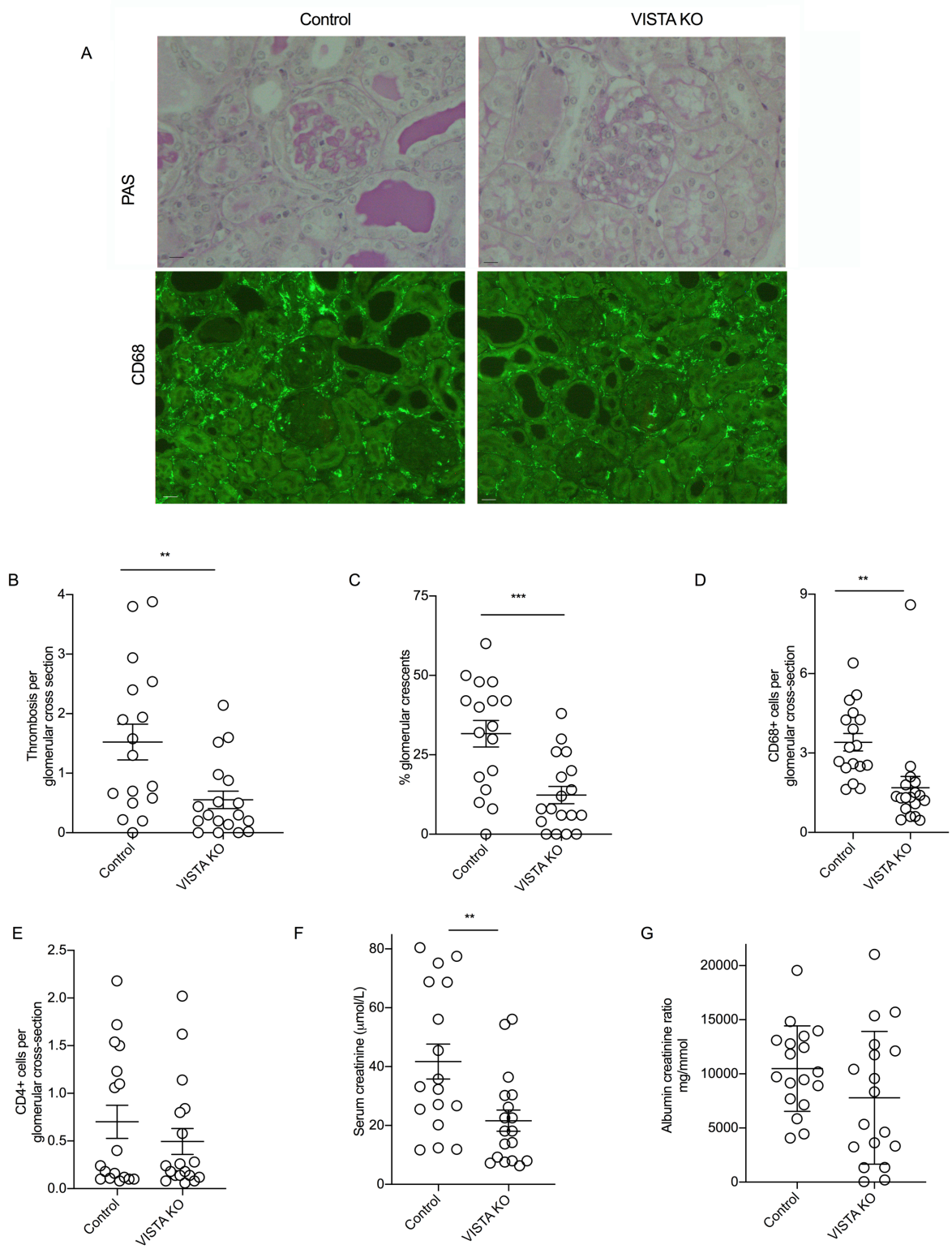

Figure 1. Autologous nephrotoxic nephritis in wild type and VISTA deficient mice with mice killed on day 7 or 8 after injection of nephrotoxic serum. Data are pooled from two experiments. (A) Representative histology showing Periodic Acid Schiff stained sections for wildtype and VISTA deficient mice at the end of the experiment. A glomerular crescent and thrombosis is seen in the wild type example. Immunofluorescence staining for CD68 positive cells. Scale bars are 10µm (PAS) and 20µm (CD68). (B-C) Quantification of thrombosis and crescents. (D-E) Glomerular CD68+ and CD4+ cells. (F-G) Biochemical parameters of disease showing serum creatinine and urine albumin creatinine ratio. Each symbol represents data from an individual mouse (mean of at least 50 glomeruli for A-B and 20 glomeruli for D-E). Error bars are mean±SEM. ** p<0.01, *** p<0.001.

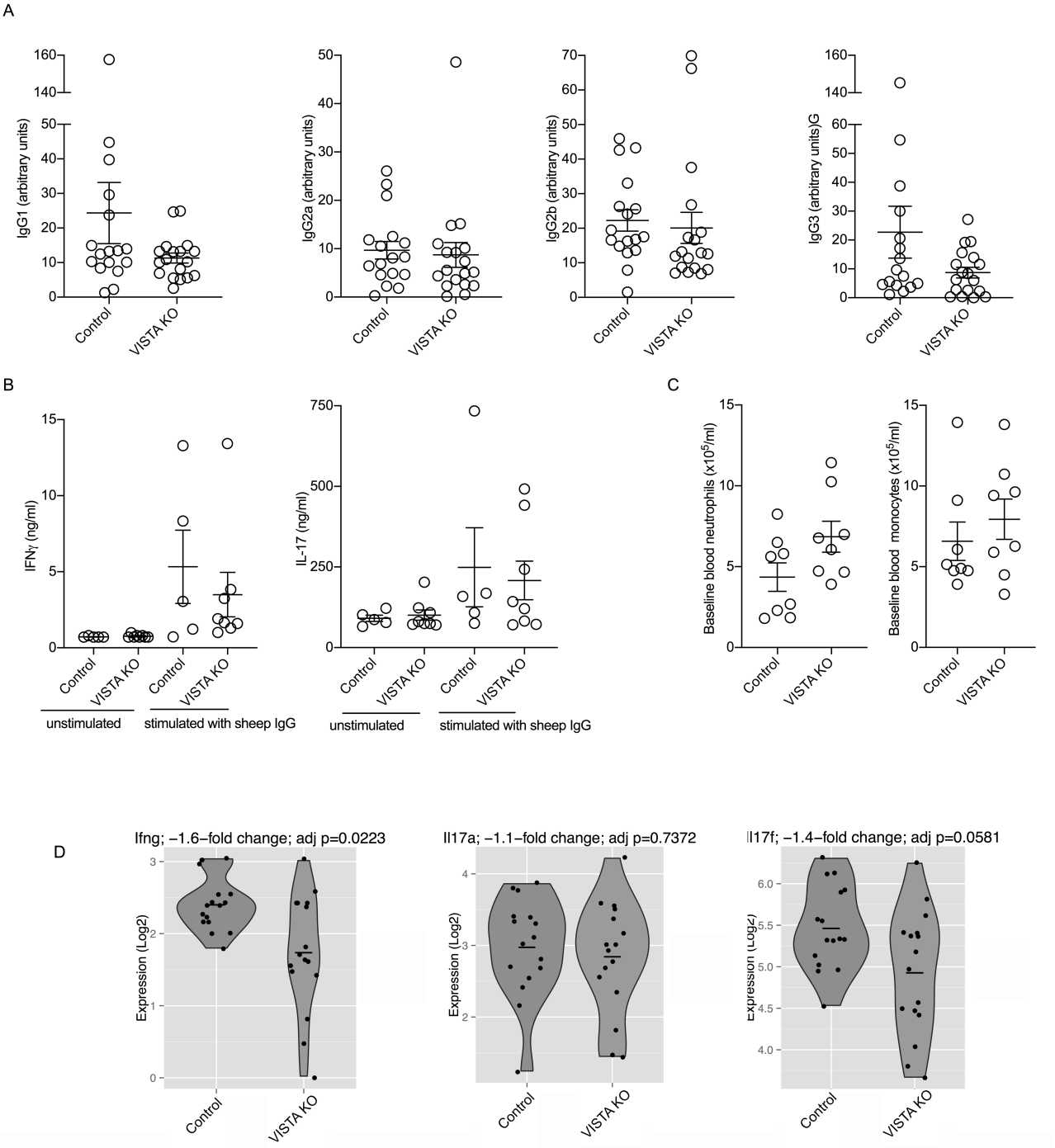

Figure 2. The immune response to sheep IgG in wild type and VISTA deficient mice. (A). Subclass specific antibodies against sheep IgG, with data pooled from two experiments. (B) IFNγ and IL-17 were measured in the supernatants of spleen cells taken at the end of one experiment and cultured with and without sheep IgG. Data are missing for one wild type mouse where a spleen was not obtained for technical reasons. (C) Peripheral blood neutrophils and monocytes in untreated wildtype and VISTA deficient mice. (D) IFNγ and IL-17A/F gene expression were measured in renal cortex from diseased animals using a nanostring assay. Data are pooled from the same two experiments shown in figure 1, with data on one mouse from each group missing for technical reasons. Each symbol represents data from an individual mouse. Error bars are mean ± SEM.

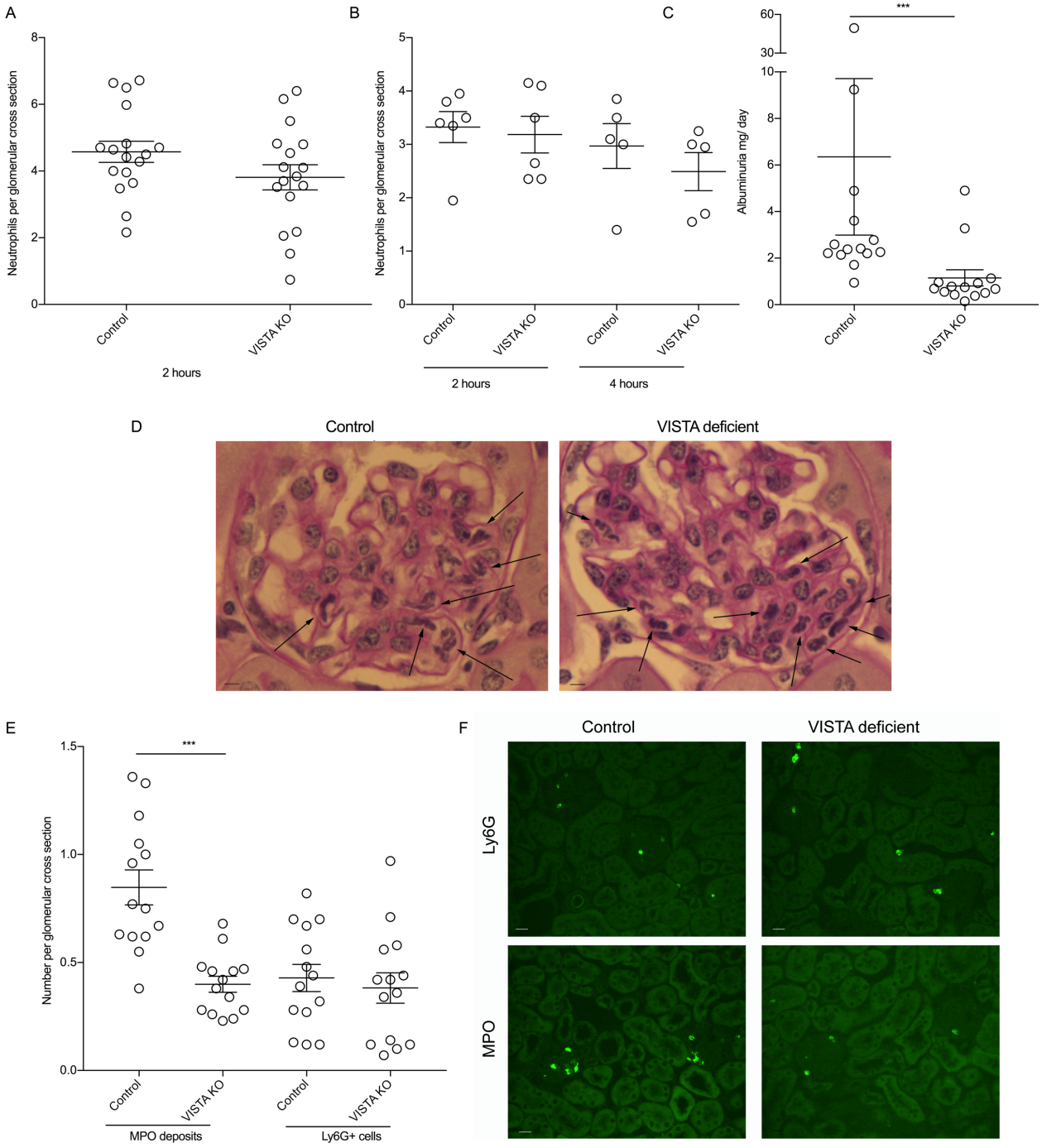

Figure 3. Heterologous nephrotoxic nephritis in wild type and VISTA deficient mice. (A) Glomerular neutrophils 2 hours after injection of nephrotoxic serum, with results pooled from 3 experiments. (B) Glomerular neutrophils at 2 and 4 hours after injection of nephrotoxic serum. (C) Albuminuria in the first 24 hours, with results pooled from 2 experiments. (D) Representative histology on PAS stained sections at 2 hours, with neutrophils shown by arrows. Scale bars are 50μm. (E) Quantification of myeloperoxidase (MPO) deposits and Ly6G+ neutrophils detected by immunofluorescence staining, with results pooled from 2 experiments. (F) Representative immunofluorescence images, with glomeruli darker than tubules due to autoflourescence on phosphate-lysine-periodate fixed tissue. Scale bars for D are 4μm and for F are 20μm. Each symbol represents data from an individual mouse (mean of at least 50 glomeruli per sample for A-B and at least 30 glomeruli per sample for E). Error bars are mean±SEM. *** p<0.001.

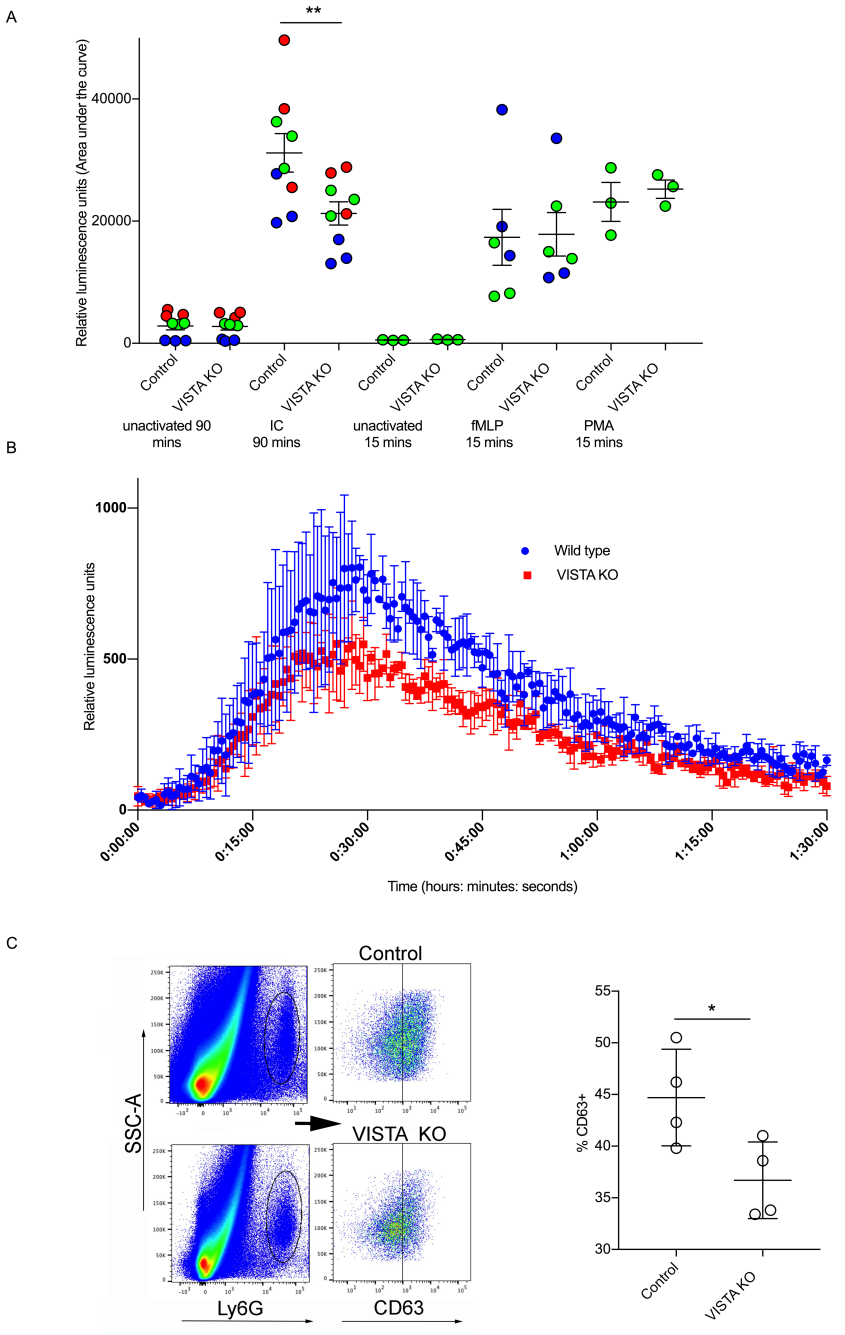

Figure 4. Neutrophil activation in wild type and VISTA deficient neutrophils. (A) Respiratory burst induced luminescence in bone marrow derived neutrophils from wild type and VISTA deficient mice stimulated with immobilised immune complexes, fMLP or PMA. Three experiments were performed. Each experiment is identified by a different colour. These data were analysed using a 2-way ANOVA. (B) Chemiluminescence over time for bone marrow neutrophils stimulated with immune complexes. Data are shown from one of the experiments in (A) with n=3 per group. (C) CD63 expression on Ly6G+ neutrophils in kidney digests at two hours after induction of heterologous nephrotoxic nephritis. In (A) and (C) each symbol represents neutrophils purified from an individual mouse. In (B) symbols are the mean of 3 individual mice per group. Error bars are mean±SEM.* $p<0.05$, ** $p< 0.001$

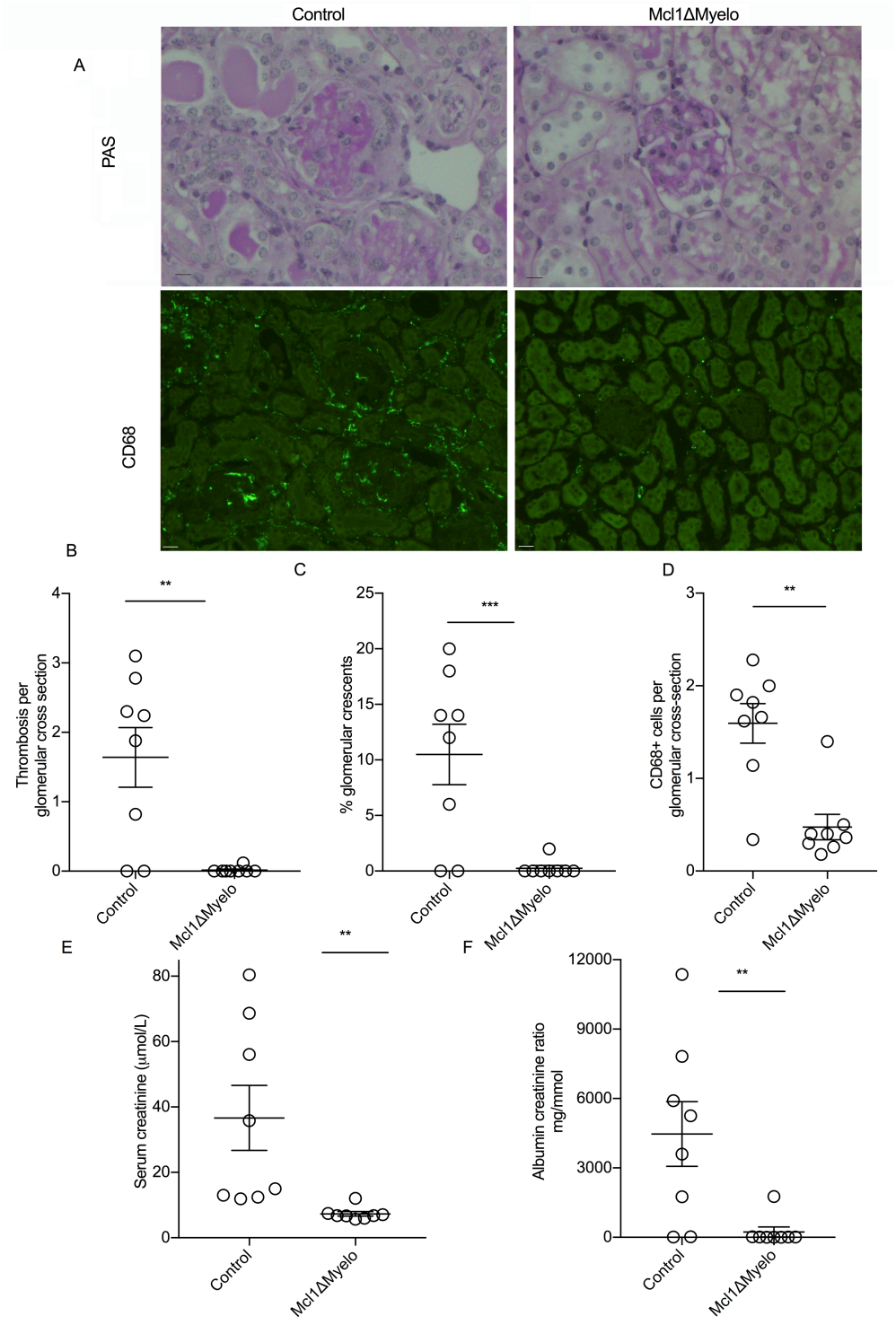

Figure 5. Autologous nephrotoxic nephritis in mice with bone marrow from control or Mcl1$^{\Delta Myelo}$ donors. The experiment ended on day 11 after injection of nephrotoxic serum. (A) Representative histology showing Periodic Acid Schiff stained sections and immunofluorescence staining for CD68 positive cells in kidney at the end of the experiment. Scale bars are 10μm (PAS) and 20μm (CD68). (B-D) Quantification of thrombosis and crescents and glomerular CD68+ cells. (E-F) Biochemical parameters of disease showing serum creatinine and urine albumin creatinine ratio. Each symbol represents data from an individual mouse (mean of at least 50 glomeruli for B-C and 20 glomeruli for D). Error bars are mean±SEM. ** p<0.01, *** p<0.001.